Electronic Supplementary Material (ESI) for Soft Matter.

Supporting Information

Modelling Network Formation in Folded Protein Hydrogels by Cluster Aggregation Kinetics

Kalila R Cook,[a] David Head,[b] and Lorna Dougan[ac]

a *School of Physics and Astronomy, Faculty of Engineering and Physical Sciences, University of Leeds, Leeds, UK.*

b *School of Computing, University of Leeds, Leeds, UK.*

c *Astbury Centre for Structural Molecular Biology, University of Leeds, Leeds, UK.*

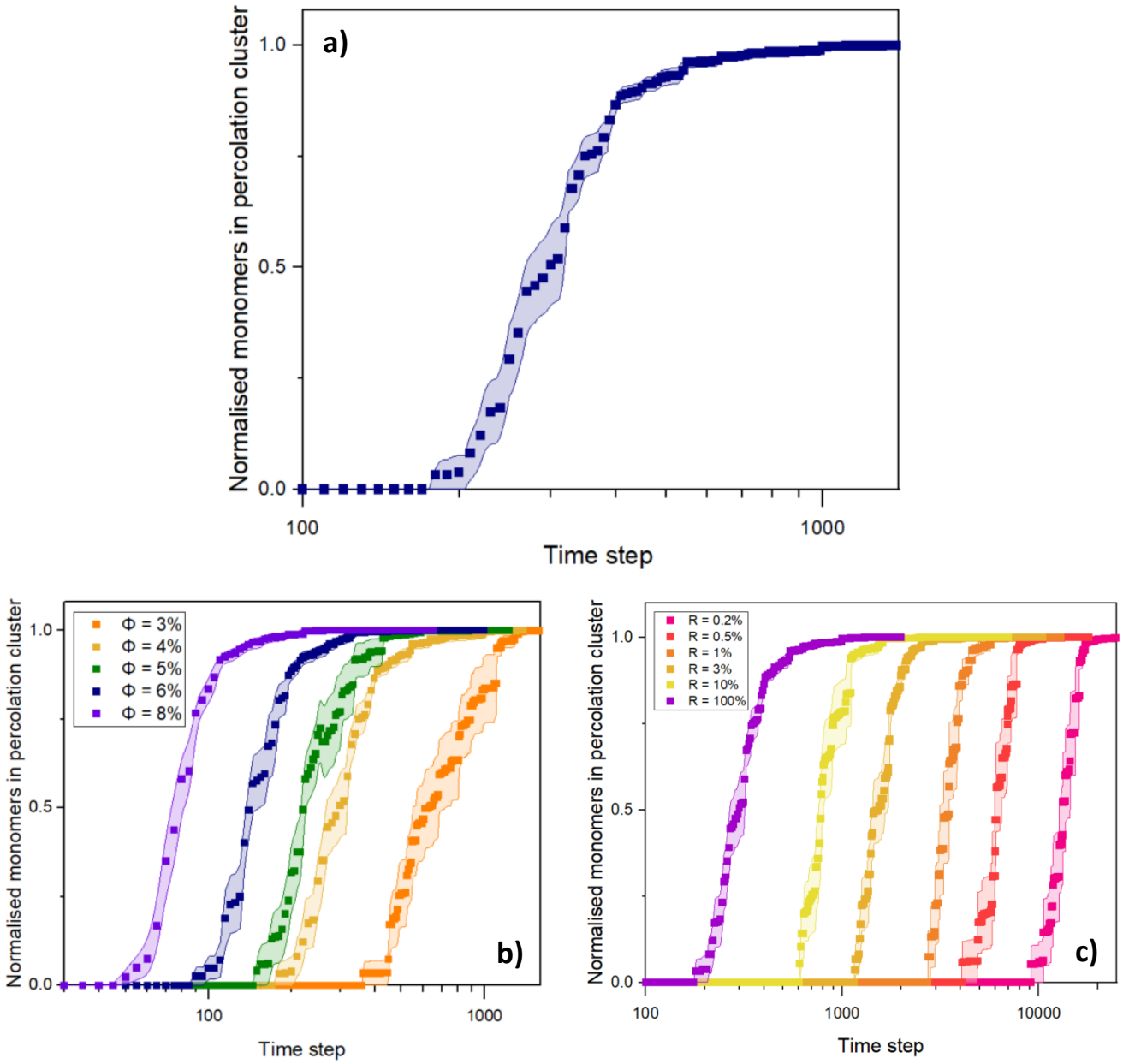

Figure S1: Plots of the change in propotion of monomers in the percolating cluster over time, with the time axis presented as logarithm base 10. a) (correlating with Fig. 1b) An example raw data curve of change in propotion of monomers in the percolating cluster over time, averaged over ten simulation runs of a 4% volume fraction system with a monomer-monomer reaction probability of 100%. b) (correlating with Fig. 2b) change in proportion of monomers in the percolating cluster over time for monomer volume fractions ranging from 3 to 8%, all for a monomer-monomer reaction probability of 100%. c) (correlating with Fig. 2c) Change in proportion of monomers in the percolating cluster over time for 4% monomer volume fraction systems ranging from 0.2 to 100% monomer-monomer reaction probabilities.

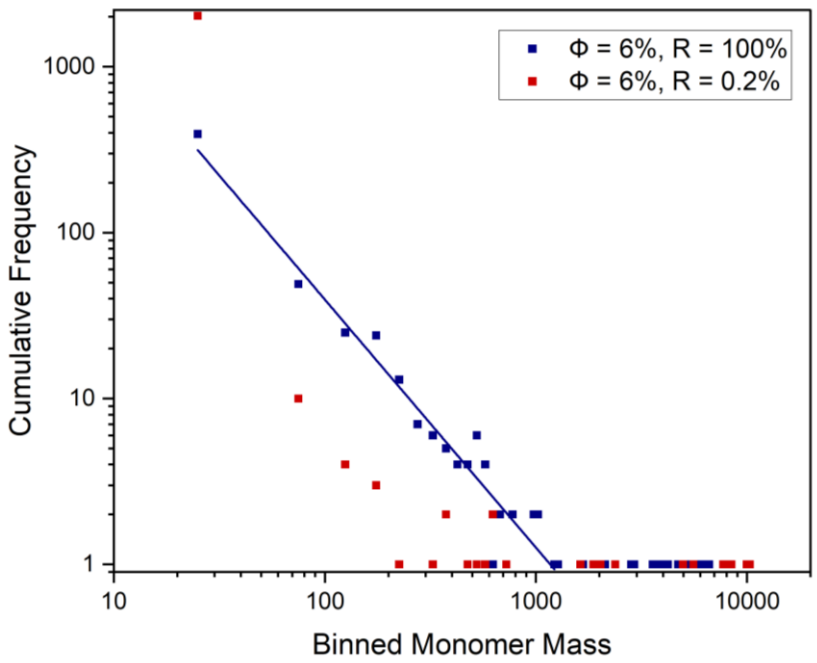

Figure S2: Cumulative frequency plot of the cluster size distribution at the percolation point for 10 runs each of a 6% monomer volume fraction system at reaction probabilities of 100 (DLCA) and 0.2% (RLCA). Cluster sizes are measured in terms of number of monomers (or monomer mass), and are binned in intervals of 50 monomers. The RLCA regime presents larger maximal clusters and many more of the smallest size clusters, with a lower frequency distribution of mid-range-size clusters than that for DLCA. A power law with exponent of -1.5 ± 0.1 is fitted to the mid-range values of the R = 100% data.

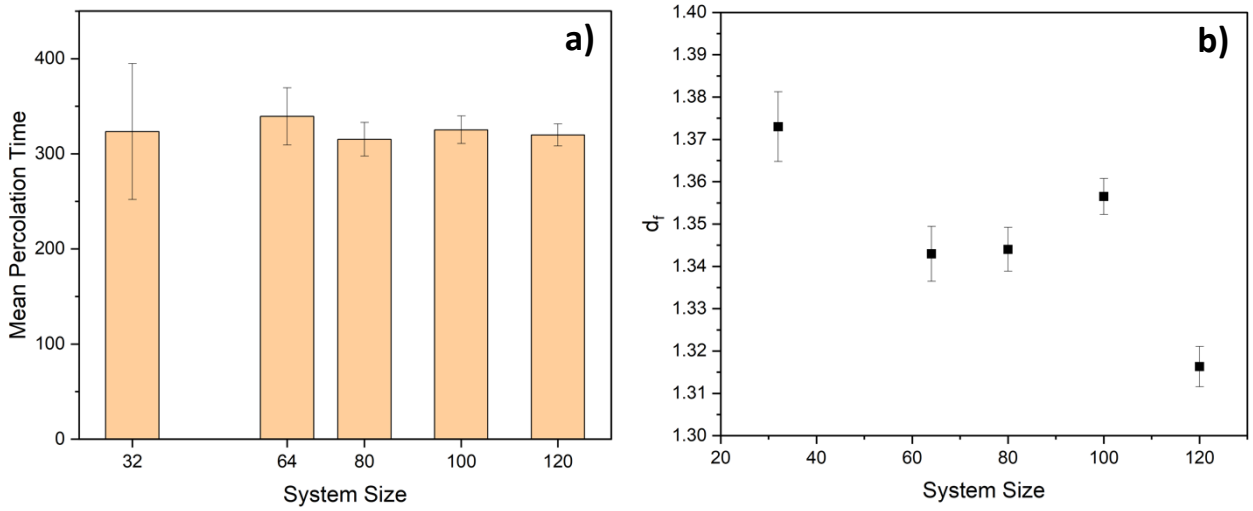

Figure S3: a) Mean percolation times and b) mean final state fractal dimensions, d_f, over 10 simulation runs each of cubic system sizes, *L*, of 32, 64, 80, 100 and 120. No variation is seen in the percolation time with *L* to within error bars. The fractal dimension values on the final system states are scattered within only 0.1 of a dimension for varied *L*. Thus the results presented in the main text are, at most, weakly dependent on finite size effects..

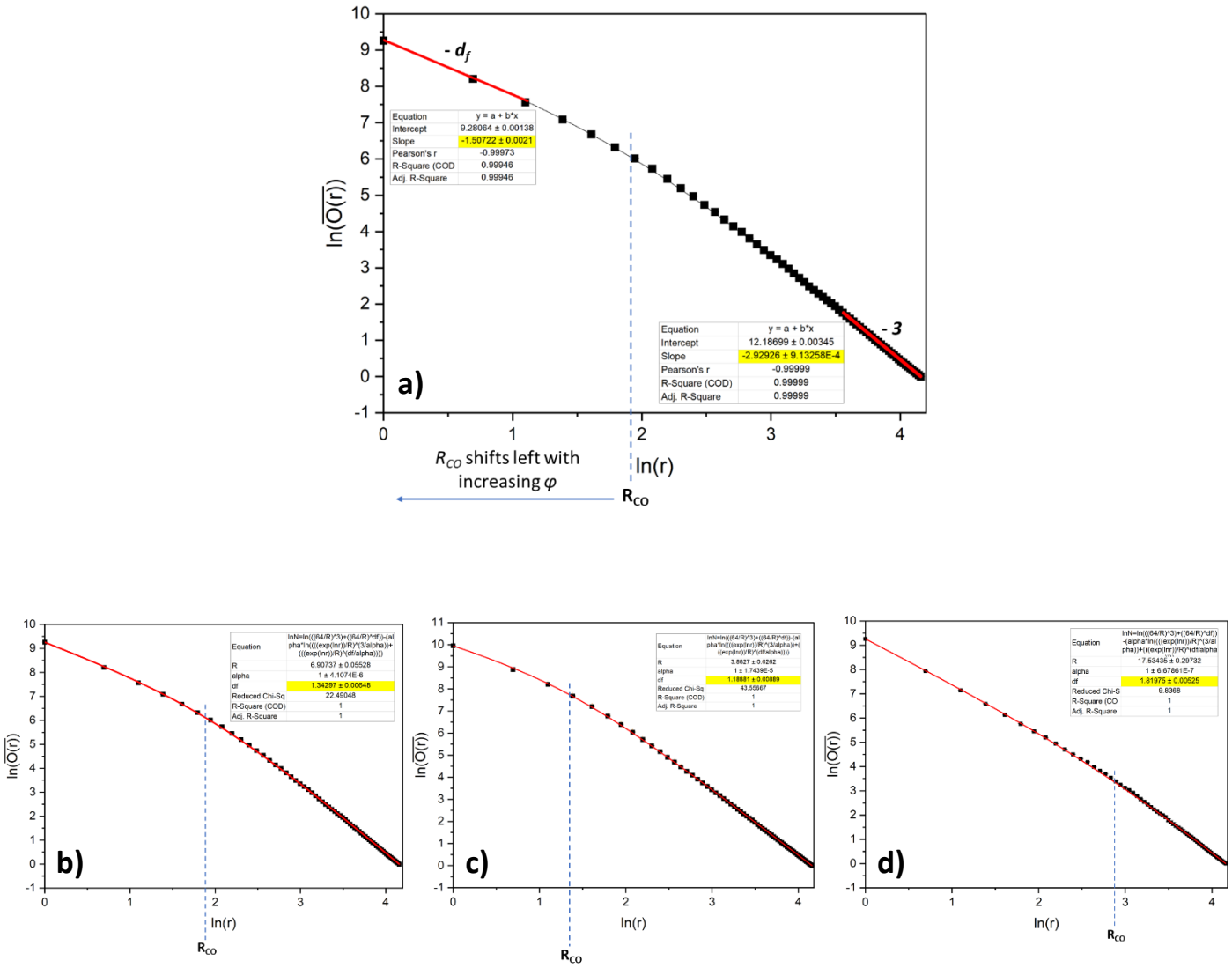

Fig S4: Exemplar box-covering data plots, showing natural logs of the occupancy number, *O(r)*, versus the box-covering measuring cube of unit size *r*. a) 4% monomer volume fraction (φ), 100% reaction probability (*R*) system. As an approximation for the fine-scale fractal dimension, a straight line is fitted at low *r*, with the slope extracted as $-d_f$ = -1.51. At high *r*, the coarse-scale fractal dimension is expected to be retrieved as -3, and our fitting of this region indeed gives -2.93. The value of *r* that is obtained as a crossover between cluster aggregation mechanisms, R_{CO}, is marked, and is noted that this crossover shifts left with increasing volume fraction. b) (φ = 4% *R* = 100%), c) (φ = 8% *R* = 100%) and d) (φ = 4% *R* = 0.2%) show data fitted with Equation 1, along with the extracted R_{CO} and values for d_f given as 1.34 ± 0.01 , 1.19 ± 0.01 and 1.82 ± 0.01, respectively.